Optical plasma diagnostics for radio-frequency ion thrusters

IEPC-2019-396

Presented at the 36th International Electric Propulsion Conference
University of Vienna, Austria
September 15-20, 2019

Benny T. Nauschütt*, Patrick Dietz†, Niklas G. Kleinmichel‡, Kristof Holste§,Hans J. Leiter¶, Peter J. Klar‖
Justus Liebig University, Giessen, 35392, Germany

This work presents the development of a method for non-invasively determining plasma parameters inside the discharge chamber of an ion thruster. Such measurements should yield valuable information during development and qualification of ion thrusters such as the 5 kW class of RITs. In conjunction with appropriate modeling, it may significantly contribute to shorter test cycles during thruster qualification as well as improvements in performance and lifetime. In our approach we measure the optical emission spectrum and the plasma parameters simultaneously. The plasma parameters can be empirically correlated with emission line ratios. In the future, these correlations will be applied to real thrusters to determine its plasma parameters truly non-invasive.

Nomenclature

p	= pressure
T_e	= electron temperature
N_e	= electron density
J_p	= ion flux
T_i	= ion temperature
N_i	= ion density
T_n	= neutral gas temperature
N_n	= neutral gas density
T	= ambient temperature
N	= total gas density
$\dot{m}$	= mass flow
L_d	= Debye length
I_sat	= saturation current
A_p	= probe surface area
m_ion	= ion mass
U	= voltage

*PhD Student, I. Physikalisches Institut, Benny.Nauschuett@physik.uni-giessen.de
†PhD Student, I. Physikalisches Institut, Patrick.Dietz@exp1.physik.uni-giessen.de
‡Master Student, I. Physikalisches Institut, Niklas.G.Kleinmichel@physik.uni-giessen.de
§Senior Researcher, I. Physikalisches Institut, Kristof.Holste@exp1.physik.uni-giessen.de
¶Professor, I. Physikalisches Institut, Hans.J.Leiter@exp1.physik.uni-giessen.de.
‖Professor, I. Physikalisches Institut, Peter.J.Klar@exp1.physik.uni-giessen.de

I. Introduction

A radio-frequency ion thruster (RIT) is operated by accelerating ions extracted from a plasma. The plasma burns inside the thruster's discharge chamber and is generated by a surrounding RF-coil[1]. Lifetime and performance strongly depend on the mode of operation, since it affects the characteristic parameters of the plasma. In a RIT, the lifetime-limiting part is the extraction grid system. It degrades during operation due to sputtering mostly induced by charge exchange[2]. A mass efficient operation can reduce charge exchange due to a lower neutral gas density, but the resulting increase in electron temperature may cause sputtering of the screen grid by the ions in the plasma due to the increased sheath potential[3]. The plasma parameters in conjunction with the grid voltages affect the function as ion optics of a grid system of defined geometry and dimensions. Thus, an exact knowledge of the plasma parameters at defined operational points of the thruster will help to optimize the grid system and to extend the thruster's lifetime.
The characteristic parameters of the plasma burning inside an operating thruster are difficult to assess without affecting the plasma itself. For example, Langmuir probes need to be inserted into the plasma during measurement. Corresponding openings are typically not available on thrusters in flight configuration. Furthermore, it is likely that the probe affects the thruster's operation.
Non-intrusive measurements using e. g. Faraday probes, retarding potential analyzers or $E \times B$-probes can be used outside the thruster in the analysis of the ion beam, but only indirectly yield information about the plasma parameters inside the thruster[4]. A promising way of non-invasively probing the plasma provides optical emission spectroscopy. However, the optical line spectra obtained need to be correlated with the plasma parameters. This usually requires a thorough theoretical modeling of the intensities of the optical transitions between the electronic states of ions and neutrals within the plasma. Corresponding models exist e. g. for argon[5] and xenon[6,7]. Alternative propellants to xenon such as iodine or krypton are of major interest[8,9], so a novel theoretical model needs to be established for each propellant. In particular, in case of molecular propellants such as iodine I_2, these models quickly become very sophisticated and require a number of microscopic parameters which have not been determined to date. This challenge can be overcome by making use of empirical correlations between optical emission spectra and plasma parameters. For this purpose we establish a data base correlating experimental spectra determined by optical emission spectroscopy and plasma parameters determined by Langmuir measurements of the same plasma.
These correlations will be used to obtain a thruster's plasma parameters only by recording its optical emission spectrum with no need for intrusive measurements. This may help gaining further insight into the internal processes within the thruster and further improving its lifetime and performance.

The experimental details are described in section II. Here, the Langmuir and optical emission spectrum measurement as well as the methods of correlating the two measurements are explained. The resulting correlations and a discussion of these are given in section III. The paper is concluded in section IV, where the method is rated and an outlook on future work is given.

II. Experimental Details

The experimental setup used is shown in Fig. 1. For the experiments, a cubic vacuum chamber with 23 cm inner edge length is used. The plasma is generated inductively by a cylindrical RF-coil (13 cm length, 8.4 cm diameter). The coil is located inside a Faraday cage that serves as a boundary for the plasma. Since the coil resides inside the cage in close contact with the plasma, the setup is different from a typical RIT. The cage can be switched between floating and grounded operation from the outside. The vertical position of the cage can be adjusted from the outside with a rotary feedthrough which is connected to the Faraday cage holders by a threaded rod. The process gas is inserted into the chamber through a tube, that ends near the Faraday cage. To achieve pressures comparable to the pressures in a RIT's discharge chamber ($p \approx 0.1\,\mathrm{Pa}$), the turbo molecular pump's pumping speed is reduced by an aperture with 15 mm diameter. The pressure is measured using a gas independent capacitive pressure probe (*Leybold CERAVAC CTR 101 N*). The process gases used were xenon and krypton.

A. Langmuir Setup

The setup for the Langmuir measurements is schematically shown on the left of Fig. 1. In this setup, a commercially available *Impedans Langmuir double probe* with built-in RF-filtering was used. Previous tests with

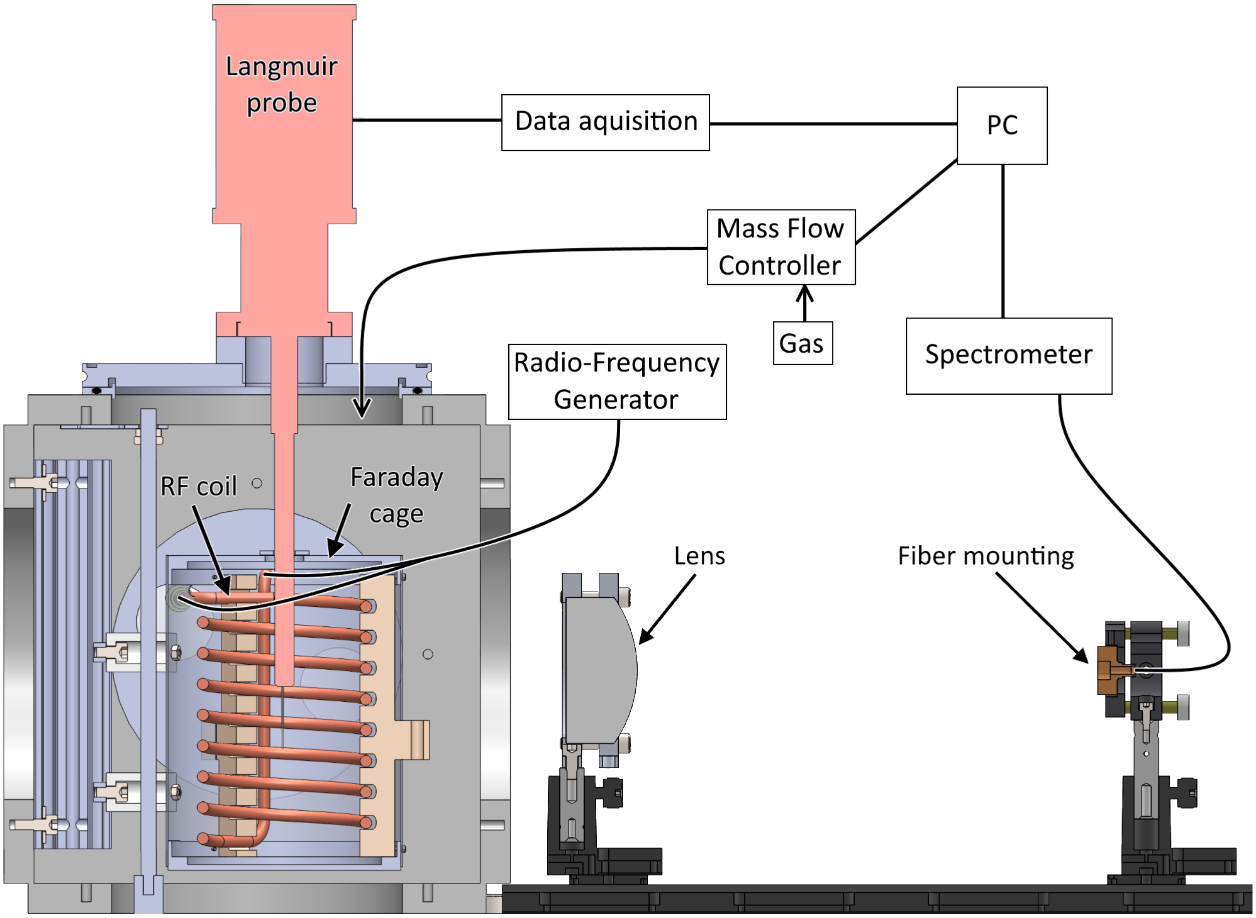

Figure 1. Setup of the experiment to correlate plasma parameters measured with a Langmuir probe and the plasma's optical emission spectrum.

a single probe were unsuccessful, since the electron saturation region could not be measured. It is assumed that by removing the electrons from the plasma, the plasma got unstable and changed properties during the measurement which caused the failure of the single probe measurement. With the double probe, no disturbances of the plasma were observed. However, the double probe assumes a Maxwell-Boltzmann distribution of the electron energies inside the plasma. In other works, it has been shown that the electron energy distributions in inductively generated plasmas may deviate from a Maxwell-Boltzmann distribution[10,11]. This means that the measured parameters are affected by a systematical error. However, in case of the typical plasma conditions inside RITs the Maxwell-Boltzmann distribution is a good approximation. It only overestimates the electron density of the higher energies. The possible deviation does not affect the outcome of our approach.

The probe is inserted into the Faraday cage from above through a circular opening with twice the diameter of the probe shaft. To seal the remaining opening in the cage's top cap, a washer with an inner diameter only slightly larger than the probe's diameter is used. The probe is located on the RF-coil's axis and therefore measures the plasma parameters in the center of the plasma. An example Langmuir measurement is shown in Fig. 2. A plasma is fully described by the following six parameters electron temperature T_e and density N_e, ion temperature T_i and density N_i and neutral gas temperature T_n and density N_n. Due to the quasi-neutrality of the plasma, electron and ion density are about equal, i. e. $N_\mathrm{e} = N\mathrm{i}$. The RF-plasma in a RIT is a low temperature plasma, thus, the ion temperature is similar to the neutral gas temperature, i. e. $T_\mathrm{i} \approx T_\mathrm{n}$, which is assumed to be comparable with the temperature of the discharge chamber T of the operating thruster. The total gas density N inside the discharge vessel can be assessed from the mass flow $\dot{m}$ for a specific thruster configuration. Due to a low ionization degree, it can be assumed that the total gas density is equal to the neutral gas density, i. e. $N = N_\mathrm{n}$, and therefore the value of the latter is known. The

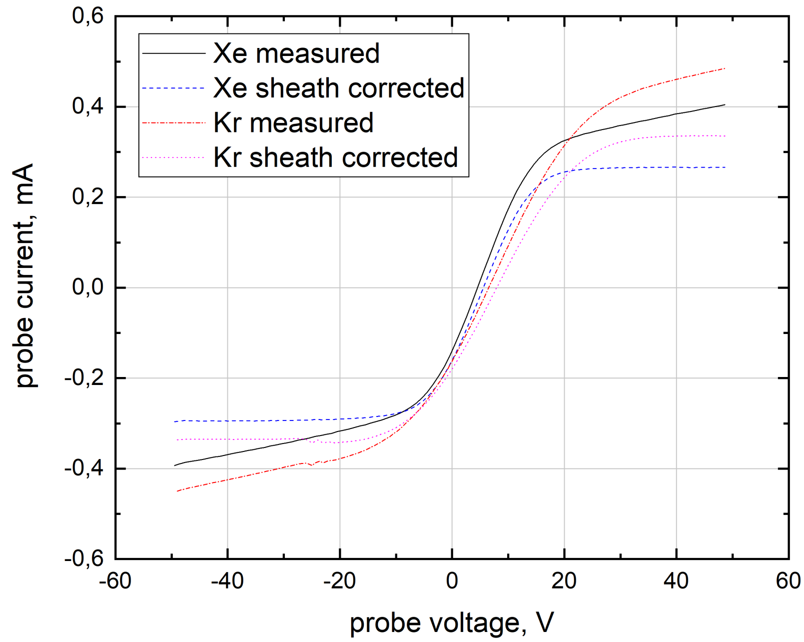

Figure 2. An example of the measured Langmuir UI-characteristics of xenon and krypton at the same pressure. The corresponding sheath expansion corrected curves are shown, too.

plasma parameters that remain unknown are therefore only the electron temperature T_e and the ion density N_i. The assumptions are summarized in Eq. 1-4.

$$p, T \text{ or } \dot{m}, \text{calculation} \rightarrow N_\mathrm{n} \tag{1}$$

$$T \rightarrow T_\mathrm{n} \approx T_\mathrm{i} \text{ (low temperature plasma)} \tag{2}$$

$$\text{Langmuir} \rightarrow N_\mathrm{i} = N_\mathrm{e} \text{ (neutrality condition)} \tag{3}$$

$$\text{Langmuir} \rightarrow T_\mathrm{e} \tag{4}$$

The parameters determined with the Langmuir double probe are electron temperature T_e, ion flux to the probe J_p, ion density N_i, plasma Debye length L_d and saturation current I_sat, which the Langmuir probe's software automatically extracts from the voltage-current-characteristic. I_sat is obtained from the sheath expansion corrected U-I-characteristics directly. T_e is calculated from the slope at $U = 0$ as shown in Eq. 5. J_p and N_i are derived from the already determined parameters and the probe surface area A_p using Eq. 6 and Eq. 7, respectively. L_d is calculated from T_e and N_i using Eq. 8 afterwards.
Thus, the equational parameters of the setup, such as gas pressure p and temperature of the discharge chamber T_n and the Langmuir parameters yield the full set of plasma parameters in conjunction with the assumptions made about the plasma regime.

$$T_\mathrm{e} = \left(\frac{2k}{e} \cdot \frac{d}{dU} \operatorname{arctanh}\left(\frac{I_\mathrm{corrected}(U)}{I_\mathrm{sat}} \right) \Bigg|_{U=0} \right)^{-1} \tag{5}$$

$$J_\mathrm{p} = \frac{I_\mathrm{sat}}{A_\mathrm{p}} \tag{6}$$

$$N_\mathrm{i} = \frac{I_\mathrm{sat}}{A_\mathrm{p} e} \sqrt{\frac{m_\mathrm{ion}}{k T_\mathrm{e}}} \tag{7}$$

$$L_\mathrm{d} = \sqrt{\frac{\epsilon_0 k T_\mathrm{e}}{e^2 N_\mathrm{i}}} \tag{8}$$

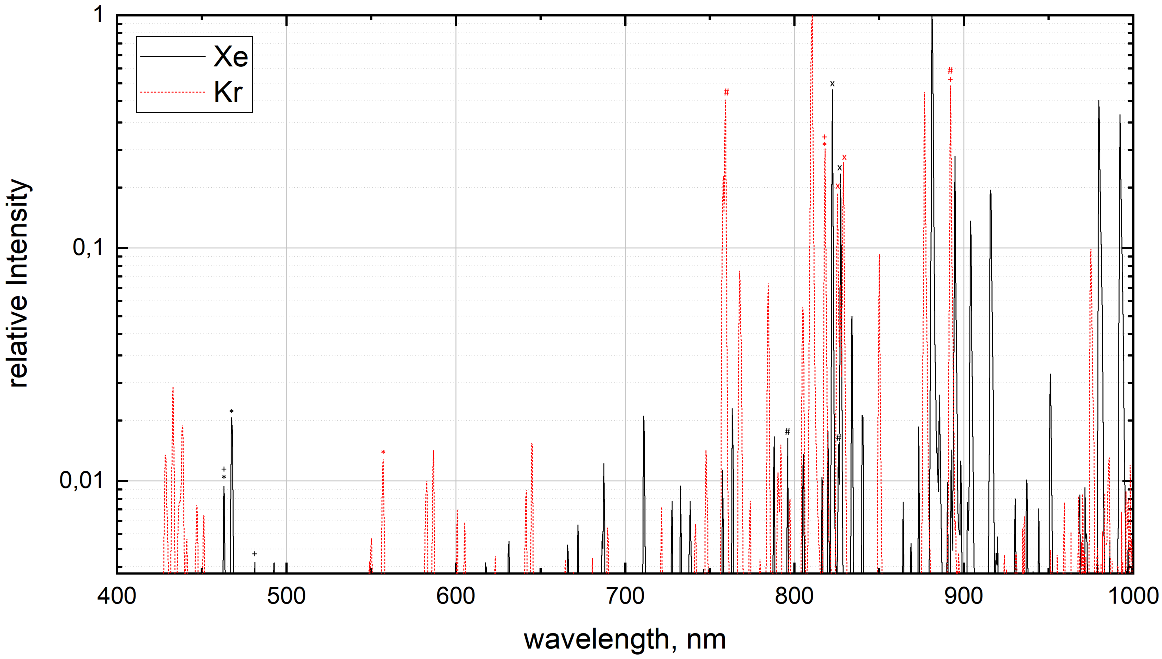

Figure 3. An example of the measured spectra of xenon and krypton at the same pressure. The emission lines that are correlated later are marked with the same symbols.

B. Optical Emission Spectroscopy Setup

The measurement setup for the optical spectroscopy is schematically shown on the right of Fig. 1. To ensure that all wavelengths are equally focused on the tip of the fiber, an achromatic lens is used. The spectrometer used was an *Ocean Optics HR2000+* with a wavelength range from 200 nm to 1100 nm. With the glass window, the lens and the fiber, the system response was determined by placing a tungsten halogen lamp of known spectrum at the position of the Faraday cage. The resulting wavelength dependent response correction function for the setup shows a steep increase at wavelengths below 400 nm. Also, the factor for wavelengths above about 1000 nm reaches 100 and increases further. This results in a high uncertainty for lines originally measured with low intensity in these regions. Therefore only a limited part of a spectrum from 400 to 1000 nm is used for the evaluation. Example spectra of xenon and krypton are shown in Fig. 3.
Once a series of measurements is acquired, a software runs all the corrections and identifies the lines in the spectra, yielding a list of wavelength and intensity data pairs.

C. Correlations

To obtain knowledge about the correlations between optical emission spectra and plasma parameters, two different algorithms were used.
Both algorithms reference a line at a certain wavelength to another line by dividing the peak intensity with the reference peak intensity. Doing this for a full series of measurements where the plasma parameters were varied systematically, the resulting ratios are used as y-axis values for the subsequent fit. We used two different approaches for generating x-axis values based on the measured plasma parameters.
The first algorithm generates the x-axis for the fit by multiplication of all measured plasma parameters, each with an exponent varying from -2 to 2 in 0.5 steps. The algorithm then iterates through all possible combinations of line ratios and exponents. Each x-y-data set is fitted with a 5th order polynomial.
The second algorithm treats each plasma parameter as a separate dimension's x-axis. The algorithm then iterates through all possible line ratios and fits each data set with a higher dimensional polynomial up to 3rd order.
The fits with the highest resulting R^2 values are identified by the software as a starting point for manual

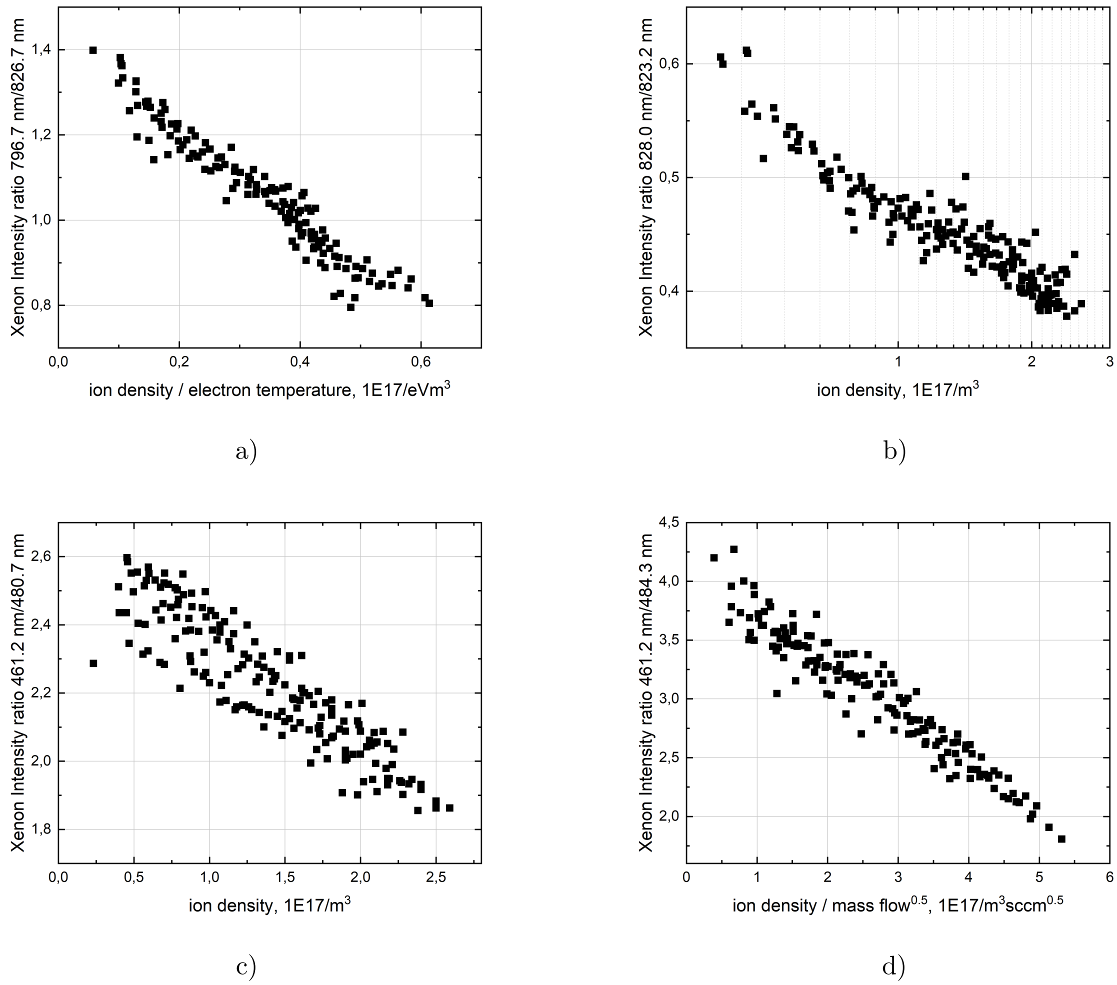

Figure 4. A selection of found correlations for xenon.

identification and verification of possible correlations.
Primarily, we need to find correlations which yield T_e and N_i when we want to replace the Langmuir probe. However, it is good to have correlations which also yield T_n and N_n as these parameters need to be estimated in a thruster otherwise.

III. Results and Discussion

Several correlations were found using the methods described above. Especially the ion density and the mass flow have a high and simple influence on most line ratios for both xenon and krypton. The notation used later (e. g. 796.7/826.7) means peak intensity of the emission line at 796.7 nm divided by the peak intensity of the reference emission line at 826.7 nm.

Some of the correlations found for xenon are shown in Fig. 4. The 796.7/826.7 intensity ratio shown in Fig. 4 a) has a linear correlation to the ratio of ion density over electron temperature. Karabadzhak found correlations of the line ratios 834.7/828.0 and 823.2/828.0 to the electron temperature using a collisional-radiative model for xenon plasma in Hall thrusters[7]. However, we could not verify these correlations in our experiments. From the two mentioned intensity ratios a correlation was found only for 823.2/828.0 to the ion density. The reciprocal correlation shown in Fig. 4 b) is exponentially decreasing. The 461.2/480.7 intensity ratio shown in Fig. 4 c) has a mostly linear correlation to the ion density. The residual deviations of the

Table 1. **Energy levels for the xenon wavelengths used for the found correlations[12].**

wavelength, nm	upper level			lower level		
	configuration	term	total angular momentum	configuration	term	total angular momentum
461.2	$5p^5(^2P^o_{3/2})7p$	$^2[3/2]$	1	$5p^5(^2P^o_{3/2})6s$	$^2[3/2]^o$	2
480.7	$5p^5(^2P^o_{3/2})7p$	$^2[1/2]$	0	$5p^5(^2P^o_{3/2})6s$	$^2[3/2]^o$	1
484.3	$5p^5(^2P^o_{3/2})7p$	$^2[3/2]$	2	$5p^5(^2P^o_{3/2})6s$	$^2[3/2]^o$	1
796.7	$5p^5(^2P^o_{3/2})7p$	$^2[3/2]$	1	$5p^5(^2P^o_{1/2})6s$	$^2[1/2]^o$	0
823.2	$5p^5(^2P^o_{3/2})6p$	$^2[3/2]$	2	$5p^5(^2P^o_{3/2})6s$	$^2[3/2]^o$	2
826.7	$5p^5(^2P^o_{1/2})6p$	$^2[1/2]$	1	$5p^5(^2P^o_{1/2})6s$	$^2[1/2]^o$	1
828.0	$5p^5(^2P^o_{3/2})6p$	$^2[1/2]$	0	$5p^5(^2P^o_{3/2})6s$	$^2[3/2]^o$	1

Table 2. **Energy levels for the krypton wavelengths used for the found correlations[13].**

wavelength, nm	upper level			lower level		
	configuration	term	total angular momentum	configuration	term	total angular momentum
583.3	$4p^5(^2P^o_{3/2})7d$	$^2[7/2]^o$	4	$4p^5(^2P^o_{3/2})5p$	$^2[5/2]$	3
760.2	$4p^5(^2P^o_{3/2})5p$	$^2[3/2]$	2	$4p^5(^2P^o_{3/2})5s$	$^2[3/2]^o$	2
819.0	$4p^5(^2P^o_{3/2})5p$	$^2[3/2]$	2	$4p^5(^2P^o_{3/2})5s$	$^2[3/2]^o$	1
826.3	$4p^5(^2P^o_{1/2})5p$	$^2[3/2]$	2	$4p^5(^2P^o_{1/2})5s$	$^2[1/2]^o$	1
829.8	$4p^5(^2P^o_{3/2})5p$	$^2[3/2]$	1	$4p^5(^2P^o_{3/2})5s$	$^2[3/2]^o$	1
892.9	$4p^5(^2P^o_{3/2})5p$	$^2[1/2]$	1	$4p^5(^2P^o_{3/2})5s$	$^2[3/2]^o$	2

data disappear, when the mass flow is used as a third dimension's axis. The result is a surface that can be described well by a three-dimensional polynomial of first order. Another linear correlation results for the intensity ratio 461.2/484.3 as a function of the ion density over the square root of the mass flow as shown in Fig. 4 d). The corresponding energy level transitions to the stated wavelengths are listed in Table 1[12].

Some of the krypton correlations found are depicted in Fig. 5. It was found, that the line ratio 819.0/583.3 increases exponentially with the product of mass flow and ion density as shown in Fig. 5 a). The line ratio 819.0/892.9 on the other hand decreases exponentially with the ratio of Debye length over mass flow, which can be seen in Fig. 5 b). The Debye length is directly dependent on the square root of the ratio of electron temperature over ion density as described by Eq. 8. Another exponentially decreasing correlation is shown in Fig. 5 c). Here, the line ratio 826.3/829.8 is correlated with the product of mass flow, electron temperature and ion density. For the line ratio 760.2/829.8 shown in Fig. 5 d), an increasing trend was found for a rising electron temperature. However, the data points are widely scattered, so another parameter might be of importance here. This trend alone is not usable to determine the electron temperature. The corresponding energy level transitions to the stated wavelengths are listed in Table 2[13].

Already with these correlations, all plasma parameters, in particular T_e and N_i, can be obtained by measuring an optical emission spectrum. Even if some correlations only yield a value that is dependent on multiple parameters, the parameters can be derived by solving a system of corresponding equations. As an example, from Fig. 4 a) the ratio of $\frac{N_\mathrm{i}}{T_\mathrm{e}}$ can be obtained from a measured intensity ratio of the xenon emission lines at 796.7 nm and 826.7 nm. By obtaining N_i from the intensity ratio of the xenon emission lines at 828.0 nm and 823.2 nm and the correlation shown in Fig. 4 b), T_e can be calculated. By using the mass flow, also the correlations shown in Fig. 4 c) and Fig. 4 d) can be utilized to obtain N_i. However, the mass flow needs to be linked to the neutral gas density for every new thruster system studied.

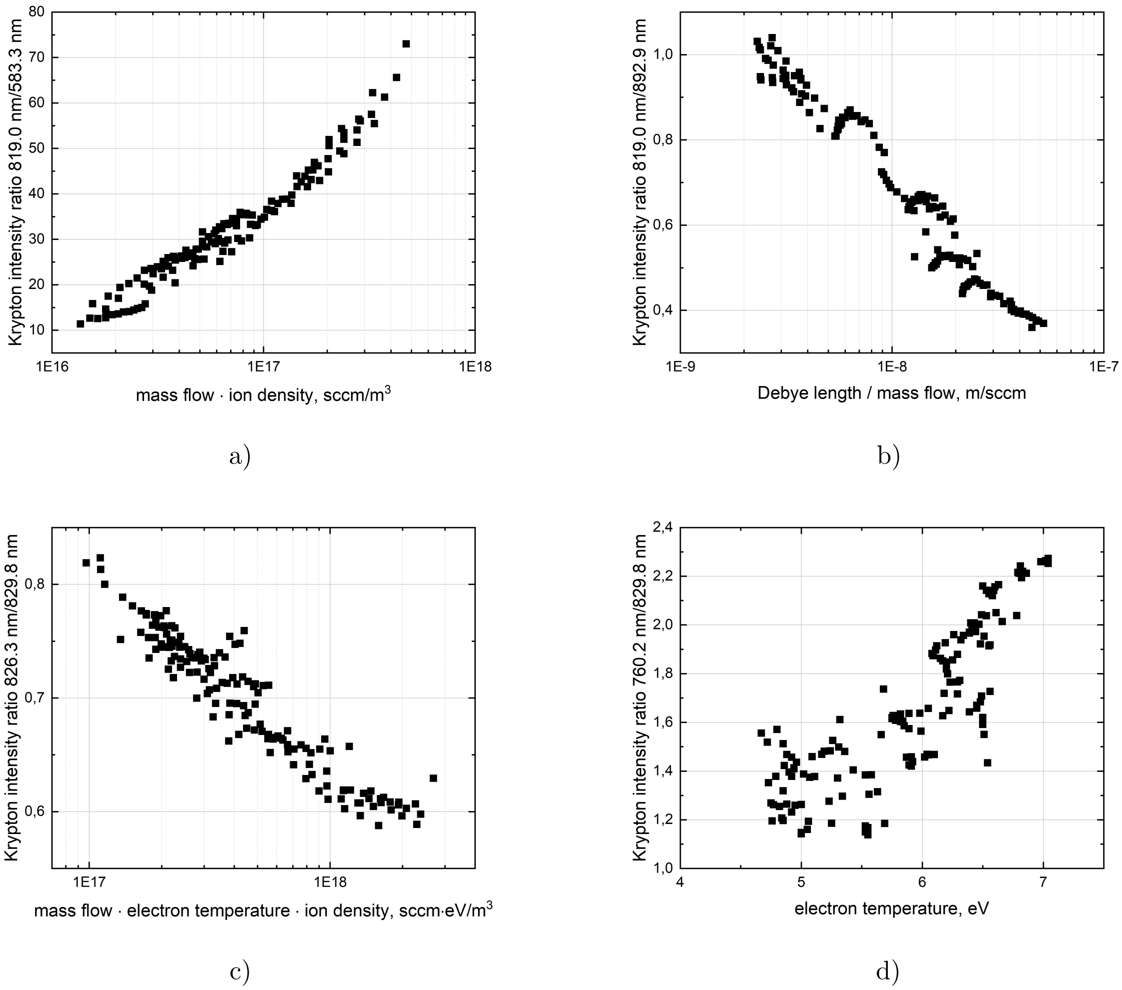

Figure 5. A selection of found correlations for krypton.

Further investigations of the correlations shown in Fig. 4 and Fig. 5 are necessary to show the underlying processes and find the correlations' origins. Deviations from the stated linear or exponential behavior may have several reasons. First, it is possible that certain parameters have smaller or larger impacts than stated. Another reason is, that a small influence of an additional parameter is neglected. This can be seen e. g. for the line ratio 461.2/480.7 in Fig. 4 c), where a small influence of the mass flow is not included in the graph. Fluctuations of the emitted light were observed sometimes, that affect the measured spectrum. These fluctuations are an indicator for plasma instabilities, that might also alter the plasma parameters measured with the Langmuir probe. For the Langmuir measurement a deviation from the expected trend can be detected during the measurement most of the times, so the scan can be repeated once the plasma is stable again. The spectrum however is recorded over a longer time (up to 1.5 minutes for low intensities), so fluctuations are hard to detect this way.

It may also be possible, that the plasma was contaminated by the evaporation of e. g. the isolation of a hot cable. This contamination might have deposited on the Langmuir probe and the glass window, which affected the resulting parameters and measured spectrum. This problem was present especially in the measurements with krypton, where the background pressure drastically changed up to a factor of 1.7 (<1.2 for xenon) depending on the input power at the same mass flow.

IV. Conclusion and next steps

Our approach for determining plasma parameters via empirical correlations from emission spectra seems viable. Our results show that enough correlations between plasma parameters and certain emission line ratios exist for both xenon as well as krypton to be able to extract the plasma parameters from the optical emission spectra based on the empirical relationships found.
However, instabilities in the plasma sometimes caused fluctuations and smaller arcs, that result in uncertainties in the optical emission spectrum. Similarly, an unstable plasma affects the Langmuir measurements. Contamination of the plasma and the Langmuir probe are also issues that need to be reduced in order to obtain more reliable measurements.

Next, we will identify the underlying processes of energy level transitions to get a deeper understanding of the correlations' origins and further validate the applicability of our approach.
Also a reliable approach to measure the electron energy distribution has to be found. Therefore the setup will be reworked, so the Langmuir single probe can be operated correctly. With the reworked setup we aim for a plasma with higher stability, so the measured plasma parameters as well as the optical spectrum can be recorded with much less disturbances.
Once the current issues with the setup are solved, the measurements will be performed again to achieve more reliable results. The found correlations will then be applied to real thrusters to determine the internal plasma parameters and open the way for further optimization of performance and lifetime.

Acknowledgments

BTN thanks *Ariane Group* for providing a PhD studentship.

References

[1] Goebel, D. M., Katz, I., "Fundamentals of Electric Propulsion: Ion and Hall Thrusters", John Wiley & Sons, Inc., Nov. 2008, ISBN: 978-0-470-42927-3, ch. 4.5

[2] Tartz, M., Hartmann, E., Neumann, H., "Evolution of Extraction Grid Erosion with Operation Lifetime", 40th Joint Propulsion Conference and Exhibit, AIAA-2004-3787, Fort Lauderdale, Florida, July 2004

[3] Sangregorio, M., Xie, K., Wang, N., Guo, N., Zhang, Z., "Ion engine grids: Function, main parameters, issues, configurations, geometries, materials and fabrication methods", CJA, **31**, 1635 (2018)

[4] Scortecci, F., Pagano, D., Bundesmann, C., Eichhorn, C., Scholze, F., Spemann, D., Leiter, H., Kersten, H., Blott, R., Mazouffre, S., Klar, P., Feili, D., Gonzales del Amo, J., "AEPD System as a Standard On-ground Tool for Electric Propulsion Thrusters", IEPC-2017-33, Oct. 2017

[5] Xi-Ming, Z., Yi-Kang, P., "Optical emission spectroscopy in low-temperature plasmas containing argon and nitrogen: determination of the electron temperature and density by the line-ratio method", J.Phys.D, **43**, 403001 (2010)

[6] Chiu, Y., Austin, B. L., Williams, S., Dressler, R. A., Karabadzhak, G. F., "Passive optical diagnostic of Xe propelled Hall thrusters. I. Emission cross sections", J. Appl. Phys., **99**, 113304 (2006)

[7] Karabadzhak, G. F., Chiu, Y. Dressler, R. A., "Passive optical diagnostic of Xe propelled Hall thrusters. II. Collisional-radiative model", J. Appl. Phys., **99**, 113305 (2006)

[8] Holste, K., Gärtner, W., Zschätzsch, D., Scharmann, S., Köhler, P., Dietz, P., Klar, P. J., "Performance of an iodine-fueled radio-frequency ion thruster", Eur. Phys. J. D, **72**, 9 (2018)

[9] Dietz, P., Gärtner, W., Koch, Q., Köhler, P. E., Teng, Y., Schreiner, P. R., Holste, K., Klar, P. J., "Molecular propellants for ion thrusters", Plasma Sources Sci. Technol., **28**, 084001 (2019)

[10] Canal, G. P., Luna, H., Galvão, R. M. O., Castell, R., "An approach to a non-LTE Saha equation based on the Druyvesteyn energy distribution function: a comparison between the electron temperature obtained from OES and the Langmuir probe analysis", J. Phys. D, **42**, 135202 (2009)

[11] Boffard, J. B., Jung, R. O., Lin, C. C., Wendt, A. E., "Optical emission measurements of electron energy distributions in low-pressure argon inductively coupled plasmas", Plasma Sources Sci. Technol., **19**, 065001 (2010)

[12] Saloman, E. B., "Energy Levels and Observed Spectral Lines of Xenon, Xe I through Xe LIV", J. Phys. Chem. Ref. Data, **33**, 765 (2004)

[13] Saloman, E. B., "Energy Levels and Observed Spectral Lines of Krypton, Kr I through Kr XXXVI", J. Phys. Chem. Ref. Data, **36**, 215 (2007)